

## Self-Assembling a Molecular Pegboard

Kyle Lund,<sup>†,§</sup> Yan Liu,<sup>§</sup> Stuart Lindsay,<sup>†,‡,§</sup> and Hao Yan<sup>\*,†,§</sup>

*Departments of Chemistry and Biochemistry, Physics, and The Biodesign Institute,  
Arizona State University, Tempe, Arizona 85287*

Received October 6, 2005; E-mail: hao.yan@asu.edu

A “molecular pegboard” that allowed specific biomolecules to be placed at specific locations with nanometer-scale accuracy would enable new types of investigation into the many processes in biology that require precise spatial positioning of cofactors. Self-assembling DNA-based nanostructures has previously been made,<sup>1</sup> and structures based on patterns of alternating tiles have been shown to bind molecules specifically.<sup>2a,1</sup> In this paper, we demonstrate the design and construction of fully addressable DNA tile nanogrids with each location bearing a unique biochemical label and show how they can be used to detect the hybridization of single DNA molecules.

Nanostructures based on the self-assembly of DNA were introduced by Seeman over 20 years ago,<sup>3</sup> and a wide variety of such structures have been produced by hybridizing DNA oligomers to form structures that contain crossover molecules.<sup>3</sup> These link adjacent double helices in a way that resembles the crossover occurring naturally in the Holliday junction.<sup>4</sup> In this way, rigid structural elements (tiles) have been constructed with mutually complementary sticky ends. These tiles assemble into arrays with repeating structural motifs, for example, as linear structures in which tiles alternate in an ABABAB... pattern. Our finite size addressable arrays are based on a recently developed cross-shaped DNA tile structure,<sup>3d</sup> which consists of four 4-arm DNA branch junctions. For the addressable array, a modified cross-shaped DNA tile structure is used (Figure 1a). Each tile has unique 7 bp sticky ends, chosen to hybridize with one, and only one other tile at each side. In addition, each tile contains a small double helical stub from which protrudes a 16 base single-stranded probe that is unique to the tile. The sequences of all single-stranded regions are chosen so as to avoid unwanted hybridizations using the SEQUIN program.<sup>5</sup> As a prototype, we assembled the 3 × 3 array of 9 tiles shown schematically in Figure 1b. We first hybridized all of the oligomers for each tile, pooled the tiles, and hybridized the mix (see Supporting Information). This stepwise assembly gave a high yield of intact arrays (>70%) by sampling and analyzing five scans each of 1 μm<sup>2</sup> area, in this analysis, the overall yield was estimated by dividing the number of intact 9 tile arrays by the total number of the arrays (intact plus smaller arrays). In the design of the addressable DNA tile array, the outer edge of each of the outer tiles had TTT overhangs that terminated further self-assembly into any larger arrays. A typical AFM image of a preparation of 9 tile arrays spread onto mica is shown in Figure 1c. The preparation has not been purified in any way and was imaged in buffer solution after a drop containing the arrays had been placed on Ni<sup>2+</sup>-treated mica<sup>6</sup> (see Supporting Information). Most (>70%) of the arrays are complete and intact. Some partly assembled arrays are visible. A gallery of magnified images of individual arrays is shown in Figure 1d. Each of the 9 tiles is clearly visible, and the structure has the expected 18 nm repeat.<sup>3d</sup>

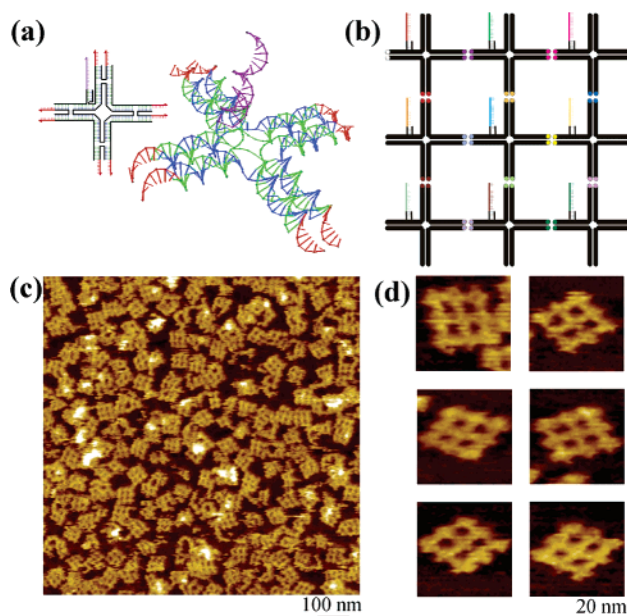


**Figure 1.** Assembly of a finite-size, chemically addressable DNA nano-array. (a) Each element is made from a cross-shaped DNA tile as shown by a planar strand pairing diagram (left) and 3D skeleton structure. (b) The 7 bp sticky ends (red) and 16 bp ssDNA tag (purple) are unique to each tile. The sticky end sequences are chosen so that each side hybridizes with one and only one partner to form a 3 × 3 array of 9 tiles. (c) The unpurified product of the hybridization reaction is shown in an AFM image. (d) A gallery of magnified images of single arrays.

To confirm the specific placement of each tile, we incorporated a biotinylated strand into certain tiles in turn, for example, the center tile, the corners, the diagonals, and the center tiles at each edge. We then incubated the arrays with streptavidin, finding bound protein only at the predicted positions (see Figure S1 in Supporting Information).

The arrays must be indexed if they are to be used as analytical devices, and the schematic arrangement of such an indexed array is shown in Figure 2a. An extra index tile has been added to the array (position “0”). We used this array to detect the hybridization of single molecules as follows. Complementary strands to the probe sequences at positions 5, 8, and 9 were biotinylated at their 3' end. The arrays were incubated with one of these three oligomers, or with a control oligomer that was also biotinylated, but not complementary to one of the probe sequences (see Supporting Information for the sequences used). After hybridization, the arrays were incubated with streptavidin, used here as a marker to label locations that acquired a biotinylated strand by hybridization (as illustrated in Figure 2b). Figure 2c–e shows AFM images demonstrating the detection of DNA hybridization to the probe at position 9, 5, and 8, respectively. The position that the streptavidin bound was evident as a white blob in the image. Statistical analysis (Table 1) shows that 64 intact arrays incubated with sequences

<sup>†</sup> Department of Chemistry and Biochemistry.

<sup>‡</sup> Department of Physics.

<sup>§</sup> The Biodesign Institute.

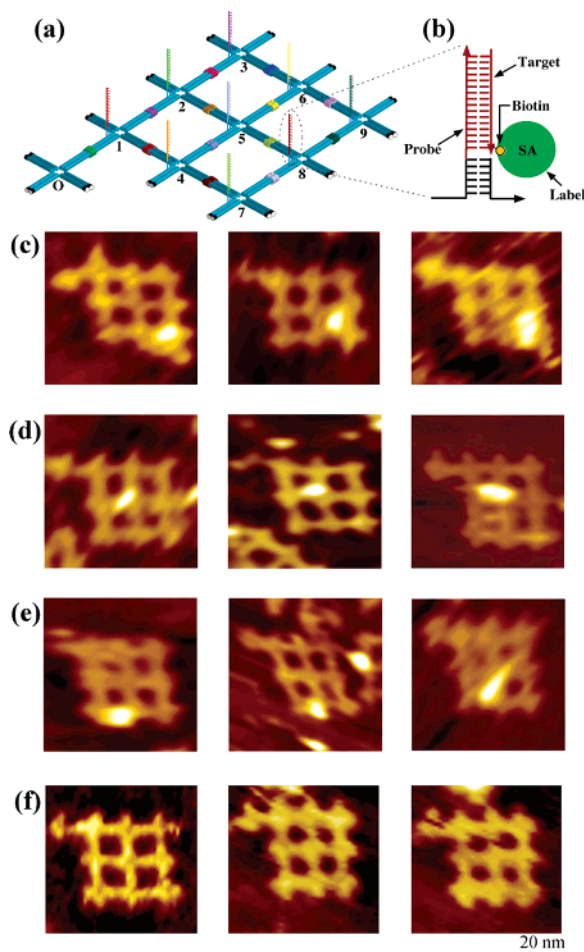


**Figure 2.** Detection of single-molecule hybridization on the nanoarray. (a) An additional tile was added to the 9-element array to serve as an index—numbers 0–9 label each tile in the array. (b) Hybridization of the probe strand with the biotinylated target strand is labeled by streptavidin binding and detected by AFM as a bright spot at the probe position. (c) AFM images with expected signals for hybridization at tile 9. (d) AFM images with expected signals for hybridization at tile 5. (e) AFM images with expected signals for hybridization at tile 8. (f) The results of a control in which the arrays were exposed to biotinylated targets that were not complementary to any of the probes are shown as magnified images.

**Table 1.**

probe location	number of 9 tiles	strand hybridization
tile 5	64	40
tile 8	54	36
tile 9	72	46
control	69	0

complementary to the probe at position 5 yielded 40 intact arrays with streptavidin at position 5 and none at other positions. Hybridization on probe 8 yielded 36 (out of 54 arrays) with bound streptavidin at position 8 and none elsewhere. Hybridization on probe 9 yielded 46 (out of 72 arrays) with bound streptavidin at position 9 and none elsewhere. In contrast, control experiments incubated with an excess of biotinylated but noncomplementary DNA yielded no streptavidin binding (see methods in Supporting Information). Figure 2f shows three examples of AFM images obtained for the control experiment. Thus, single-molecule hybridization was detected on these arrays with an average efficiency of 64%.

From our previous experience with AFM imaging of streptavidin-labeled 2D DNA arrays,<sup>21</sup> the streptavidin molecules positioned on

the array appear as higher topographical features no matter whether the streptavidin is above or below the DNA lattice. In this work, the flexibility of the protruding DNA stub may cause the streptavidin sitting near the cavities of the DNA grid instead of overlapping exactly with DNA, and this can be seen in some of the AFM images shown in Figure 2. Thus, the measured labeling efficiencies quoted above are indicative of the overall efficiency of hybridization and streptavidin labeling. As a further control, we examined arrays that were hybridized with complementary target DNA but that were not streptavidin labeled (data not shown). High-resolution images showed some changes (possibly owing to an increased stiffness in the hybridized strands vs the ssDNA) but no evidence of the white blobs that mark the streptavidin binding in these images.

Even these small ( $3 \times 3$ ) arrays should prove useful for probing cooperative interactions between pairs of tethered peptides, by investigating cooperative effects in ligand binding, for example. The array would permit 12 possible pairs of nearest neighbor interactions to be probed, enough to try out all 10 possible pairings of five distinct peptides. A small-scale addressable array may also find applications in investigating proximity effect between proteins or other macromolecules. By increasing the length of the sticky ends to allow more space for unique sequence designs, there appears to be no fundamental limit to the size of the array that could be built, so long as it was assembled in sequential steps to minimize the amount of partially hybridized product. For example, an array with  $1 \mu\text{m}$  on each side would require  $\sim 2500$  tiles and  $\sim 2 \times 10^4$  unique sticky ends. In this scenario, a string of 9 bases will provide  $4^9$  unique sticky end choices, which are enough to build a  $1 \mu\text{m}^2$  array. Nevertheless, error correction mechanisms<sup>7</sup> are needed for constructing large arrays. Fully addressable nanoarrays of this kind will open an entirely new vista in molecular assembly and the analysis of spatial interactions between diverse biologically relevant molecules.

**Acknowledgment.** This work has been supported by grants from the NSF and a grant from the Biodesign Institute at ASU to H.Y. and S.L.

**Supporting Information Available:** DNA sequences, experimental methods, additional AFM images. This material is available free of charge via the Internet at <http://pubs.acs.org>.

## References

- (1) Seeman, N. C. *Nature* **2003**, *421*, 427–431.
- (2) (a) Winfree, E.; Liu, F.; Wenzler, L. A.; Seeman, N. C. *Nature* **1998**, *394*, 539–544. (b) LaBean, T. H.; Yan, H.; Kopatsch, J.; Liu, F.; Winfree, E.; Reif, J. H.; Seeman, N. C. *J. Am. Chem. Soc.* **2000**, *122*, 1848–1860. (c) Mao, C.; Sun, W.; Seeman, N. C. *J. Am. Chem. Soc.* **1999**, *121*, 5437–5443. (d) Yan, H.; Park, S. H.; Finkelstein, G.; Reif, J. H.; LaBean, T. H. *Science* **2003**, *301*, 1882–1884. (e) Liu, D.; Wang, M.; Deng, Z.; Walulu, R.; Mao, C. *J. Am. Chem. Soc.* **2004**, *126*, 2324–2325. (f) Ding, B.; Sha, R.; Seeman, N. C. *J. Am. Chem. Soc.* **2004**, *126*, 10230–10231. (g) Rothmund, P. W. K.; Papadakis, N.; Winfree, E. *PLoS Biology* **2004**, *2*, 2041–2053. (h) Shih, W. M.; Quispe, J. D.; Joyce, G. F. *Nature* **2004**, *427*, 618–621. (i) Malo, J.; Mitchell, J. C.; Venien-Bryan, C.; Harris, J. R.; Wille, H.; Sherratt, D. J.; Turberfield, A. *J. Angew. Chem., Int. Ed.* **2005**, *44*, 3057–3061. (j) Mathieu, F.; Liao, S.; Kopatsch, J.; Wang, T.; Mao, C.; Seeman, N. C. *Nano Lett.* **2005**, *5*, 661–665. (k) Park, S. H.; Barish, R.; Li, H.; Reif, J. H.; Finkelstein, G.; Yan, H.; LaBean, T. H. *Nano Lett.* **2005**, *5*, 693–696. (l) Park, S. H. et al. *Nano Lett.* **2005**, *5*, 729–733. (m) Chworos, A.; Severcan, I.; Koefman, A. Y.; Weinkam, P.; Oroudjev, E.; Hansma, H. G.; Jaeger, L. *Science* **2004**, *306*, 2068–2072. (n) Chelyapov, N.; Brun, Y.; Gopalkrishnan, M.; Reishus, D.; Shaw, B.; Adleman, L. *J. Am. Chem. Soc.* **2004**, *126*, 13924–13925.
- (3) Seeman, N. C. *J. Theor. Biol.* **1982**, *99*, 237–247.
- (4) Holliday, R. *Genet. Res.* **1964**, *5*, 282–304.
- (5) Seeman, N. C. *J. Biomol. Struct. Dyn.* **1990**, *8*, 573–581.
- (6) Hansma, H. G.; Laney, D. E. *Biophys. J.* **1996**, *70*, 1933–1939.
- (7) Winfree, E.; Bekbolatov, R. DNA Computing, Lecture Notes in Computer Science. **2004**, *2943*, 126–144.

JA0568446